Circulation

ORIGINAL RESEARCH ARTICLE

Increased Reactive Oxygen Species–Mediated Ca²⁺/Calmodulin-Dependent Protein Kinase II Activation Contributes to Calcium Handling Abnormalities and Impaired Contraction in Barth Syndrome

BACKGROUND: Mutations in tafazzin (*TAZ*), a gene required for biogenesis of cardiolipin, the signature phospholipid of the inner mitochondrial membrane, causes Barth syndrome (BTHS). Cardiomyopathy and risk of sudden cardiac death are prominent features of BTHS, but the mechanisms by which impaired cardiolipin biogenesis causes cardiac muscle weakness and arrhythmia are poorly understood.

METHODS: We performed in vivo electrophysiology to define arrhythmia vulnerability in cardiac-specific *TAZ* knockout mice. Using cardiomyocytes derived from human induced pluripotent stem cells and cardiac-specific *TAZ* knockout mice as model systems, we investigated the effect of *TAZ* inactivation on Ca²⁺ handling. Through genome editing and pharmacology, we defined a molecular link between *TAZ* mutation and abnormal Ca²⁺ handling and contractility.

RESULTS: A subset of mice with cardiac-specific *TAZ* inactivation developed arrhythmias, including bidirectional ventricular tachycardia, atrial tachycardia, and complete atrioventricular block. Compared with wild-type controls, BTHS-induced pluripotent stem cell–derived cardiomyocytes had increased diastolic Ca²⁺ and decreased Ca²⁺ transient amplitude. BTHS-induced pluripotent stem cell–derived cardiomyocytes had higher levels of mitochondrial and cellular reactive oxygen species than wild-type controls, which activated CaMKII (Ca²⁺/calmodulin-dependent protein kinase II). Activated CaMKII phosphorylated the RYR2 (ryanodine receptor 2) on serine 2814, increasing Ca²⁺ leak through RYR2. Inhibition of this reactive oxygen species–CaMKII–RYR2 pathway through pharmacological inhibitors or genome editing normalized aberrant Ca²⁺ handling in BTHS-induced pluripotent stem cell–derived cardiomyocytes and improved their contractile function. Murine *Taz* knockout cardiomyocytes also exhibited elevated diastolic Ca²⁺ and decreased Ca²⁺ transient amplitude. These abnormalities were ameliorated by Ca²⁺/calmodulin-dependent protein kinase II or reactive oxygen species inhibition.

CONCLUSIONS: This study identified a molecular pathway that links *TAZ* mutation with abnormal Ca²⁺ handling and decreased cardiomyocyte contractility. This pathway may offer therapeutic opportunities to treat BTHS and potentially other diseases with elevated mitochondrial reactive oxygen species production.

Xujie Liu, PhD
Suya Wang, PhD
Xiaoling Guo, PhD
Yifei Li, MD, PhD
Roza Ogurlu, BS
Fujian Lu, PhD
Maksymilian Prondzynski, PhD
Sofia de la Serna Buzon, PhD
Qing Ma, MD
Donghui Zhang, PhD
Gang Wang, MD, PhD
Justin Cotton, BS
Yuxuan Guo, PhD
Ling Xiao, PhD
David J. Milan, MD, PhD
Yang Xu, PhD
Michael Schlame, MD
Vassilios J. Bezzerides, MD, PhD
William T. Pu, MD

https://www.ahajournals.org/journal/circ

Clinical Perspective

What Is New?

- *TAZ* mutant hearts are vulnerable to complete heart block and ventricular tachycardia.
- *TAZ*-deficient cardiomyocytes have abnormal Ca²⁺ handling.
- A reactive oxygen species (ROS)–CaMKII (Ca²⁺/calmodulin-dependent protein kinase II)–RYR2 (ryanodine receptor 2) molecular pathway links *TAZ* mutation to abnormal Ca²⁺ handling in Barth syndrome (BTHS) induced pluripotent stem cell–derived cardiomyocytes, which contributes to decreased cardiomyocyte contractile function.

What Are the Clinical Implications?

- Evaluation of patients with BTHS for ventricular tachycardia and dynamic heart block is warranted.
- Abnormal Ca²⁺ handling observed in BTHS induced pluripotent stem cell–derived cardiomyocytes may contribute to cardiac dysfunction and arrhythmia in patients with BTHS.
- Manipulation of the identified ROS–CaMKII–RYR2 pathway offers therapeutic opportunities for BTHS and potentially other forms of heart disease with elevated mitochondrial reactive oxygen species production.

Cardiolipin, the signature phospholipid of the inner mitochondrial membrane, is required for the normal function of enzymes housed within this structure, most notably the electron transport chain and F1F0 ATP synthase.[1,2] Altered cardiolipin abundance and composition in heart failure have been hypothesized to impair mitochondrial function and contribute to cardiac dysfunction.[3,4] Study of Barth syndrome (BTHS), the only known inherited disorder of cardiolipin metabolism, has provided critical insights into the biological function of cardiolipin. BTHS is caused by mutation of the X-linked gene tafazzin (*TAZ*),[5] which encodes a mitochondrial phospholipid-lysophospholipid transacylase responsible for the terminal step in the biogenesis of cardiolipin.[6] The major clinical features of BTHS are cardiac and skeletal myopathy and neutropenia. Cardiomyopathy and sudden cardiac death are among the major clinical features that affect patient quality of life and survival.[7–9]

The molecular mechanisms that connect *TAZ* deficiency with cardiomyopathy and sudden death are not clearly defined. Previously, we integrated human induced pluripotent stem cell (iPSC)–derived cardiomyocytes (iPSC-CMs), genome editing, and heart-on-a-chip technologies to model the cardiomyopathy of BTHS in a dish. We demonstrated that BTHS iPSC-CMs had high levels of reactive oxygen species (ROS),[10] which was

confirmed in *TAZ*-deficient murine cardiomyocytes.[11] BTHS iPSC-CM–based muscular thin films had impaired force generation, which was normalized by suppression of elevated ROS using the mitochondrially targeted ROS scavenger MitoTEMPO.[10]

Intracellular Ca²⁺ is a critical regulator of cardiac rhythm and contraction. During the cardiomyocyte action potential, the L-type Ca²⁺ channel in the plasma membrane opens and allows entry of extracellular Ca²⁺. This increase in cytoplasmic Ca²⁺ opens ryanodine receptor 2 (RYR2), located on the sarcoplasmic reticulum (SR), resulting in Ca²⁺-induced Ca²⁺ release. The subsequent rapid increase in intracellular Ca²⁺ triggers sarcomere contraction. Inactivation of the L-type Ca²⁺ channel, closure of RYR2, and return of Ca²⁺ to the SR, through the activity of SERCA2a (sarcoplasmic/endoplasmic reticulum Ca²⁺-ATPase 2a), and the extracellular space, via NCX1 (Na⁺/Ca²⁺ exchanger), restores Ca²⁺ to its normal low levels in diastole, leading to sarcomere relaxation and preparing the cell for the next excitation-contraction cycle. Abnormal Ca²⁺ handling can impair cardiac contraction and relaxation and potentially precipitate lethal arrhythmias.[12]

Here we tested the hypothesis that impaired Ca²⁺ handling contributes to cardiac dysfunction and arrhythmia in BTHS by studying BTHS iPSC-CMs. We found that BTHS iPSC-CMs have reduced Ca²⁺ transient amplitude and elevated diastolic Ca²⁺. We linked these abnormalities with excessive mitochondrial ROS production through activation of Ca²⁺/calmodulin-dependent protein kinase II (CaMKII) and phosphorylation of RYR2 serine 2814 (RYR2-S2814). Last, we demonstrate that inhibition of this ROS-CaMKII-RYR2 pathway ameliorated the abnormal Ca²⁺ handling and weak contraction of BTHS iPSC-CMs. Studies on murine *Taz* knockout cardiomyocytes confirmed that these mechanisms are operative in bona fide cardiomyocytes. These results provide new insights into the links among mitochondrial dysfunction, ROS, abnormal Ca²⁺ handling, cardiac muscle weakness, and arrhythmia and identify novel therapeutic avenues for BTHS.

METHODS

All supporting data are available within the article and the Expanded Methods in the Data Supplement.

iPSC Culture, Differentiation, and Treatment

PGP1 is a wild-type human male iPSC line that harbors a doxycycline-inducible CRISPR/Cas9 transgene.[10,13] BTHH was derived from PGP1 using doxycycline-induced Cas9 genome editing[13] to introduce a *TAZ* frameshift mutation (c.517delG) found in a BTHS patient.[10,13] This patient's cells were also reprogrammed to yield an iPSC line, pBTHH.[10] The

doxycycline-induced Cas9 genome editing strategy was used to introduce the same *TAZ* frameshift mutation into PGP1 harboring RYR2-S2814A (serine 2814 to alanine) mutations in both alleles[14] (herein named WT-S2814A), yielding BTHH-S2814A. Sequences and primers used in this study are provided in Table I in the Data Supplement. Normal karyotype was validated by either G-banded karyotyping or Nanostring karyotype assay (Figure IA in the Data Supplement).

Cardiomyocyte differentiation was induced as described previously[15,16] with minor modifications (Figure IB in the Data Supplement). iPSC-CM purity was measured by flow cytometry and immunofluorescent staining using primary antibodies shown in Table II in the Data Supplement.

Ca²⁺ Imaging

For ratiometric Ca^{2+} imaging, iPSC-CMs loaded with Fura-2 AM (Life Technologies) were recorded under 1-Hz pacing using the IonOptix Myocyte Calcium and Contractility System. The change in the Fura-2 signal after the addition of 10 mM caffeine was used to measure SR Ca^{2+} content. SR Ca^{2+} leak was measured as the tetracaine-induced reduction of the Fluo-3 AM signal, as described previously.[17] For nonratiometric Ca^{2+} imaging, cells were programmed to express the GCaMP6f-Junctin Ca^{2+} nanosensor, expressed from an adenovirus,[18] or GCaMP5 lentivirus (Addgene No. 46027)[19] and recorded by confocal line scan imaging (Olympus FV3000) or a Vala Biosciences Kinetic Image Cytometer.

Protein Expression

Proteins were analyzed using the WES capillary Western system (ProteinSimple). Primary antibodies are shown in Table II in the Data Supplement. HRP-conjugated secondary antibodies were from ProteinSimple. Total RYR2 was measured by ELISA (LifeSpan BioSciences, Inc).

Contractility Measurement

Engineered heart tissues (EHTs) were generated from iPSC-CMs (1E6 cells per EHT) as described[20] using iPSC-CMs treated with adenovirus that expressed ChR2-YFP.[14] EHTs were optically paced at 1 Hz at 37 °C and recorded at 30 frames per second using a Keyence BZ-X Fluorescence Microscope with a ×2 objective. Videos were analyzed using MuscleMotion.[21]

Taz Knockout Mice and Murine Cardiomyocytes

Animal experiments were performed following protocols approved by Boston Children's Hospital Animal Care and Use Care Committee. Electrophysiology studies were performed as described previously.[22] *Taz^{flox/flox}* mice on a C57BL/6J background were described previously.[23] Neonatal cardiomyocytes were isolated and purified using kits from Miltenyi Biotec. Cells were treated with adenovirus expressing either LacZ (Ad:LacZ; control) or Cre (Ad:Cre; *Taz* knockout).[24] *Taz^{flox/Y}; Myh6-Cre* (cardiomyocyte-specific *Taz* knockout, CKO) and *Taz^{WT/Y}; Myh6-Cre* (control) mice were used for adult cardiomyocyte isolation by retrograde collagenase perfusion.[25]

Statistical Analysis

Results are displayed as mean±SD. Normally distributed data were analyzed with Welch 2-tailed *t* test (2 groups) or ANOVA with Dunnett post hoc test (≥3 groups). Otherwise, we used the Kruskal–Wallis test with the Dunn post hoc test or a permutation test. Values of $P<0.05$ were considered significant.

RESULTS

In Vivo Arrhythmias in *Taz* Cardiac Knockout Mice

Patients with BTHS are at risk for sudden death.[7–9] Arrhythmia mechanisms are not well described, although case reports suggest vulnerability to ventricular tachycardia (VT).[26] To better characterize arrhythmia vulnerability in *TAZ* deficiency, we performed electrophysiology studies on mice with cardiac-specific *Taz* inactivation (CKO) at 6 weeks of age (Figure 1A), when they had mild or no cardiac dysfunction[27] (Figure IIA in the Data Supplement). Six of 9 CKO mice had arrhythmias (Figure 1B–1D): 2 developed progressive atrioventricular node dysfunction that culminated in lethal complete heart block (Figure IIB in the Data Supplement); 2 developed bidirectional VT after adrenergic stimulation; 1 developed induced VT; and 1 developed induced atrial tachycardia. Among littermate controls, 2 of 8 developed induced VT, which had a much shorter duration than VT in CKO mice (Figure 1E). The overall frequency of arrhythmias was greater in CKO, and, despite the small sample size and transient induced VT in 2 controls, this difference trended toward statistical significance (permutation test, $P=0.096$). These results suggest that cardiac *Taz* deficiency increases vulnerability to different types of arrhythmias. We were particularly interested in the vulnerability to bidirectional VT given that this is an uncommon arrhythmia most closely linked to digitalis toxicity and catecholaminergic VT,[28] conditions that both involve elevated cytosolic Ca^{2+}.

iPSC-CM Differentiation and Metabolic Characterization

iPSCs were efficiently differentiated to yield >70% TNNT2⁺ (Troponin T Type 2) iPSC-CMs (Figure IB–ID in the Data Supplement), which exhibited robust contraction and Ca^{2+} transients (Video I in the Data Supplement). Most iPSC-CMs expressed ventricular cardiomyocyte marker MLC2V (HUGO Gene Nomenclature Committee: Myosin Light Chain 2) and not immature or atrial cardiomyocyte marker MLC2A (HUGO Gene Nomenclature Committee: MYL7; Figure IE in the Data Supplement). The wild-type male human iPSC line PGP-1 was used as wild-type control (WT), and the PGP1-TAZ^{c.517delG} line,[10] generated from PGP-1 by genome editing (Figure IIIA in the Data Supplement),
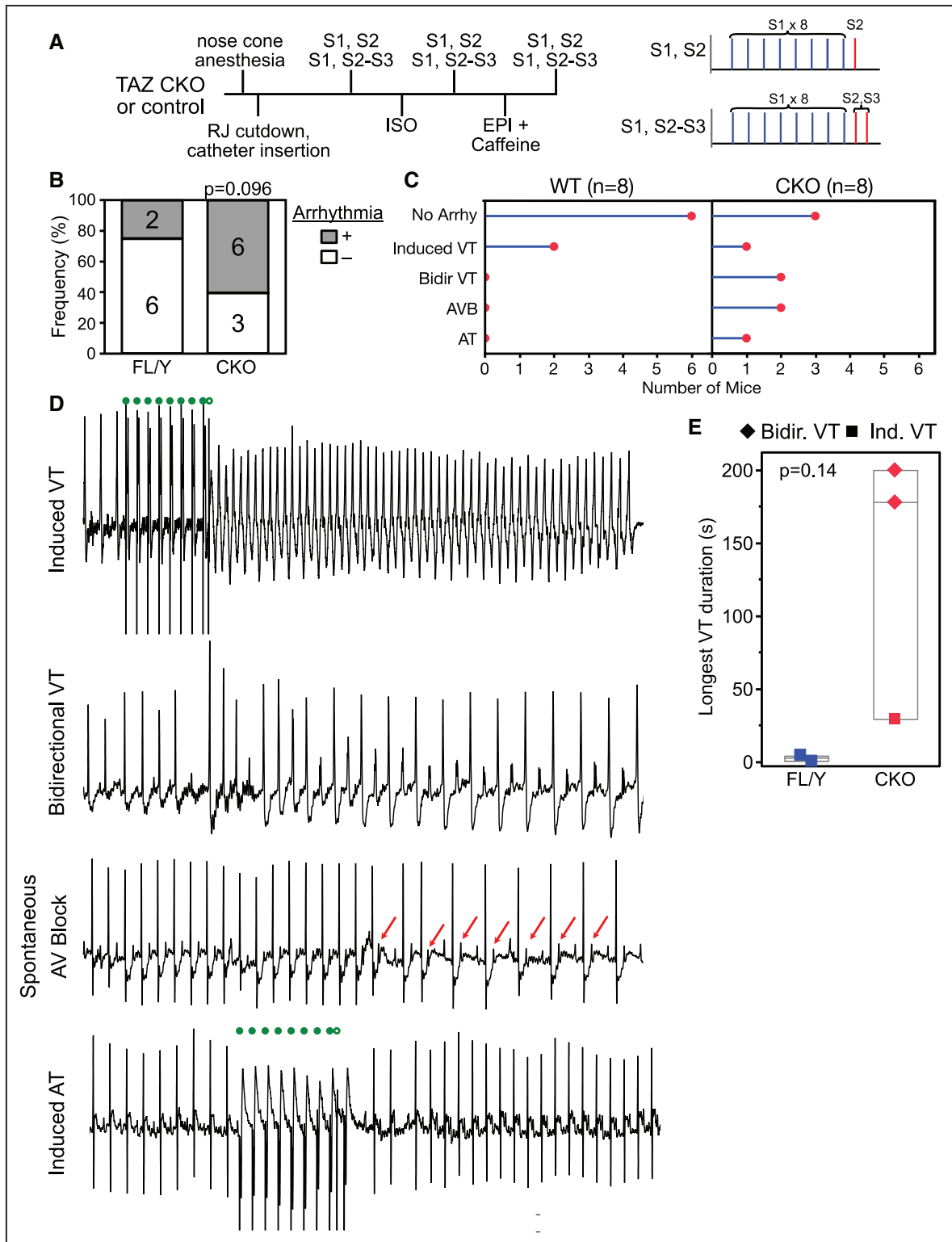
Figure 1. Cardiac arrhythmias in *Taz* cardiac-specific knockout mice.
Male control (*Taz^FL/Y*) or cardiac-specific mutant mice (CKO, *Myh6-Cre*; *Taz^FL/Y*) underwent intracardiac electrophysiology study at 6 weeks of age. Studies and analyses were performed blinded to genotype. **A**, Schematic of electrophysiology study protocol. **B**, Fraction of mice with arrhythmia. Numbers indicate sample sizes. Permutation test. **C**, Classification of types of arrhythmia within each genotype. **D**, Representative surface electrocardiograms demonstrating types of arrhythmias observed in CKO. • and ○ green circles indicate S1 to S2 programmed ventricular stimulation. Red → highlights nonconducted p-waves. Bidirectional VT was induced by treatment with epinephrine and caffeine. **E**, Longest duration of VT. VT duration was greater in CKO mice, although this was not statistically significant at these low sample sizes. Permutation test. CKO indicates cardiac-specific *Taz* inactivation; TAZ, tafazzin; and VT, ventricular tachycardia.

was used as the *TAZ* mutant line (BTHH). Sanger sequencing confirmed the single base pair frameshift mutation in the *TAZ* gene of BTHH (Figure IIIB in the Data Supplement), and capillary Western demonstrated absence of TAZ protein in BTHH iPSC-CMs (Figure IIIC in the Data Supplement). Lipid mass spectrometry confirmed abnormal cardiolipin composition in BTHH iPSC-CMs (Figure IIID in the Data Supplement). Mitochondrial networks, visualized by mitotracker green, demonstrated reduced branching number and branch length in BTHH iPSC-CMs compared with WT (Figure IIIE and IIIF in the Data Supplement). Mitochondrial function, measured using an extracellular flux analyzer, was impaired in BTHH iPSC-CMs (Figure IIIG and IIIH in the Data Supplement).

BTHH iPSC-CMs Exhibit Abnormal Ca²⁺ Handling

To assess Ca^{2+} handling in BTHH iPSC-CMs, we loaded iPSC-CMs with the Ca^{2+} indicator Fura-2 and performed ratiometric Ca^{2+} imaging under electric pacing at 1 Hz. Compared with WT, BTHH iPSC-CMs Ca^{2+} transient amplitude was lower by 30%, and the diastolic Ca^{2+} concentration was higher by 34% (Figure 2A–2C). The maximal upstroke and recovery velocities of BTHH Ca^{2+} transients were significantly depressed compared with control (Figure 2D and 2E). Similar abnormal Ca^{2+} handling was also observed in pBTHH iPSC-CMs, derived from a BTHS patient (Figure IVA in the Data Supplement).

Diastolic Ca^{2+} leak through RYR2, the major cardiomyocyte intracellular Ca^{2+} release channel, is a key determinant of cytoplasmic diastolic Ca^{2+} concentration. We quantified diastolic Ca^{2+} leak through RYR2 using the previously described "tetracaine shift" assay.[17] This showed that the diastolic Ca^{2+} leak through RYR2 was significantly greater in BTHH iPSC-CMs compared with WT (Figure IVB in the Data Supplement).

Increased Ca^{2+} leak through RYR2 often produces spontaneous Ca^{2+} release events known as *Ca²⁺ sparks*. To corroborate our finding of increased RYR2 Ca^{2+} leak, we measured Ca^{2+} sparks by using adenovirus to express a genetically encoded Ca^{2+} nanosensor, in which GCaMP6f is fused to Junctin, a protein that colocalizes with RYR2 in cardiomyocytes.[18] BTHH iPSC-CMs exhibited more frequent Ca^{2+} sparks (Figure 2F and 2G). To better define the prevalence of aberrant Ca^{2+} release events, we used a higher-throughput Ca^{2+} imaging system to record Ca^{2+} transients in a larger number of cells. The results confirmed that a much larger fraction of BTHH iPSC-CMs exhibited abnormal Ca^{2+} release events during pacing or immediately after pacing (Figure IVC–IVF in the Data Supplement).

Increased diastolic SR Ca^{2+} leak and reduced Ca^{2+} transient amplitude suggested the possibility of depleted SR Ca^{2+} stores. To test this hypothesis, after a standard pacing protocol, iPSC-CMs were treated with caffeine, which opens RYR2 and rapidly empties SR Ca^{2+} stores. BTHH iPSC-CMs showed significantly reduced caffeine-induced Ca^{2+} release compared with isogenic control iPSC-CMs (Figure 2H and 2I), suggesting reduced SR Ca^{2+} stores.

ROS Links *TAZ* Mutation to Abnormal Ca²⁺ Handling in BTHH iPSC-CMs

We aimed to delineate mechanisms by which deficiency of TAZ, a mitochondrial protein, induced elevated SR Ca^{2+} leak through RYR2. We showed previously that BTHS iPSC-CMs have elevated levels of mitochondrial ROS,[10] and we hypothesized that high ROS levels in BTHS iPSC-CMs may contribute to abnormal Ca^{2+} handling.

We first confirmed that BTHH iPSC-CMs have elevated ROS by using flow cytometry to measure the mean fluorescence intensity of BTHH and WT mitochondria isolated from iPSC-CMs and stained with MitoSOX, a mitochondrially targeted, fluorescent ROS indicator (Figure 3A). Elevated ROS was also detected at the level of whole cells in BTHH iPSC-CMs stained with CellROX, a whole-cell fluorescent ROS probe (Figure 3B). Consistent with these measurements, BTHH iPSC-CMs had elevated levels of 4-hydroxynonenal, a product of lipid peroxidation (Figure 3C).

We next tested whether elevated ROS contributes to impaired Ca^{2+} handling in BTHH iPSC-CMs. To reduce ROS, we treated cells with the mitochondrially targeted ROS scavenger MitoTEMPO. MitoTEMPO reduced ROS in BTHH iPSC-CMs (Figure 3D). We then analyzed the effect of MitoTEMPO on iPSC-CM Ca^{2+} handling. MitoTEMPO treatment significantly improved Ca^{2+} transient amplitude and normalized diastolic Ca^{2+} concentration in BTHH iPSC-CMs (Figure 3E and 3F). However, the Ca^{2+} transient maximal upstroke and recovery velocities were not significantly changed (Figure 3G and 3H). MitoTEMPO also reduced the high Ca^{2+} spark frequency observed in BTHH iPSC-CMs (Figure IVG in the Data Supplement). For comparison, we treated cells with *TAZ* modified mRNA (*TAZ* modRNA), which we showed previously rescues *TAZ* mutant iPSC-CM metabolic, structural, and contractile phenotypes.[10] *TAZ* modRNA corrected Ca^{2+} amplitude, diastolic Ca^{2+} concentration, and Ca^{2+} transient maximum upstroke velocity so that they were not significantly different between BTHH and WT (Figure 3E–3G), although it did not significantly correct the Ca^{2+} transient maximum recovery velocity (Figure 3H). These data demonstrate that ROS is an essential intermediate that links TAZ deficiency with abnormal Ca^{2+} handling in BTHH iPSC-CMs. Less complete rescue by MitoTEMPO compared with *TAZ* modRNA suggests that either MitoTEMPO incompletely suppressed excessive ROS levels or that both ROS-dependent and non–ROS-dependent mechanisms contribute to the phenotype of *TAZ* mutant cells.
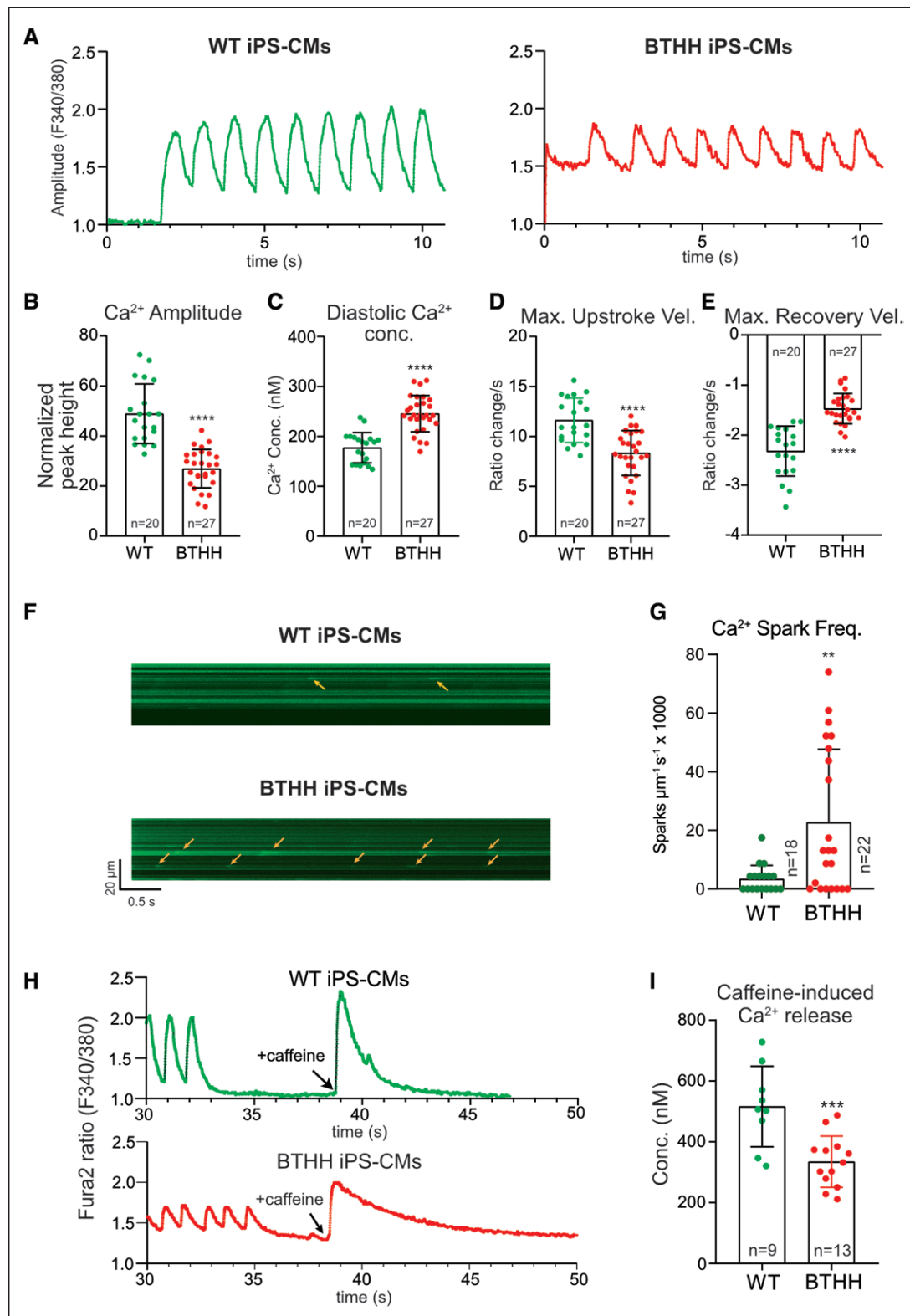
Figure 2. Abnormal Ca²⁺ handling in BTHH iPSC-CMs.

A, Representative Ca²⁺ transients of WT and BTHH iPSC-CMs imaged by Fura-2. Cells were electrically paced at 1 Hz. **B** through **E**, Quantitative analysis of the Ca²⁺ transient amplitude, diastolic Ca²⁺ concentration, and maximal Ca²⁺ upstroke and recovery velocities of WT and BTHH iPSC-CMs paced at 1 Hz. Each dot represents a different cell cluster. **F** and **G**, Ca²⁺ sparks in BTHH and WT iPSC-CMs cells. iPSC-CMs expressing a GCaMP6f-Junctin Ca²⁺ nanosensor[18] were paced at 1 Hz. Ca²⁺ sparks were recorded by confocal line scan imaging (**F**). Yellow →, Ca²⁺ sparks. Quantitative analysis (**G**) showed that Ca²⁺ spark frequency was significantly higher in BTHH compared with WT. n indicates number of cells studied. **H** and **I**, Sarcoplasmic reticulum Ca²⁺ stores were measured by quantifying caffeine-induced Ca²⁺ release in Fura-2–loaded iPSC-CMs. **H**, representative Ca²⁺ transient traces of caffeine-induced Ca²⁺ transient. **I**, quantitative analysis of caffeine-induced Ca²⁺ release in BTHH compared with WT. Two-tailed *t* test: ****P*<0.01, *****P*<0.001, ******P*<0.0001. BTHH indicates Barth syndrome; iPSC-CM, induced pluripotent stem cell–derived cardiomyocyte; and WT, wild-type control.
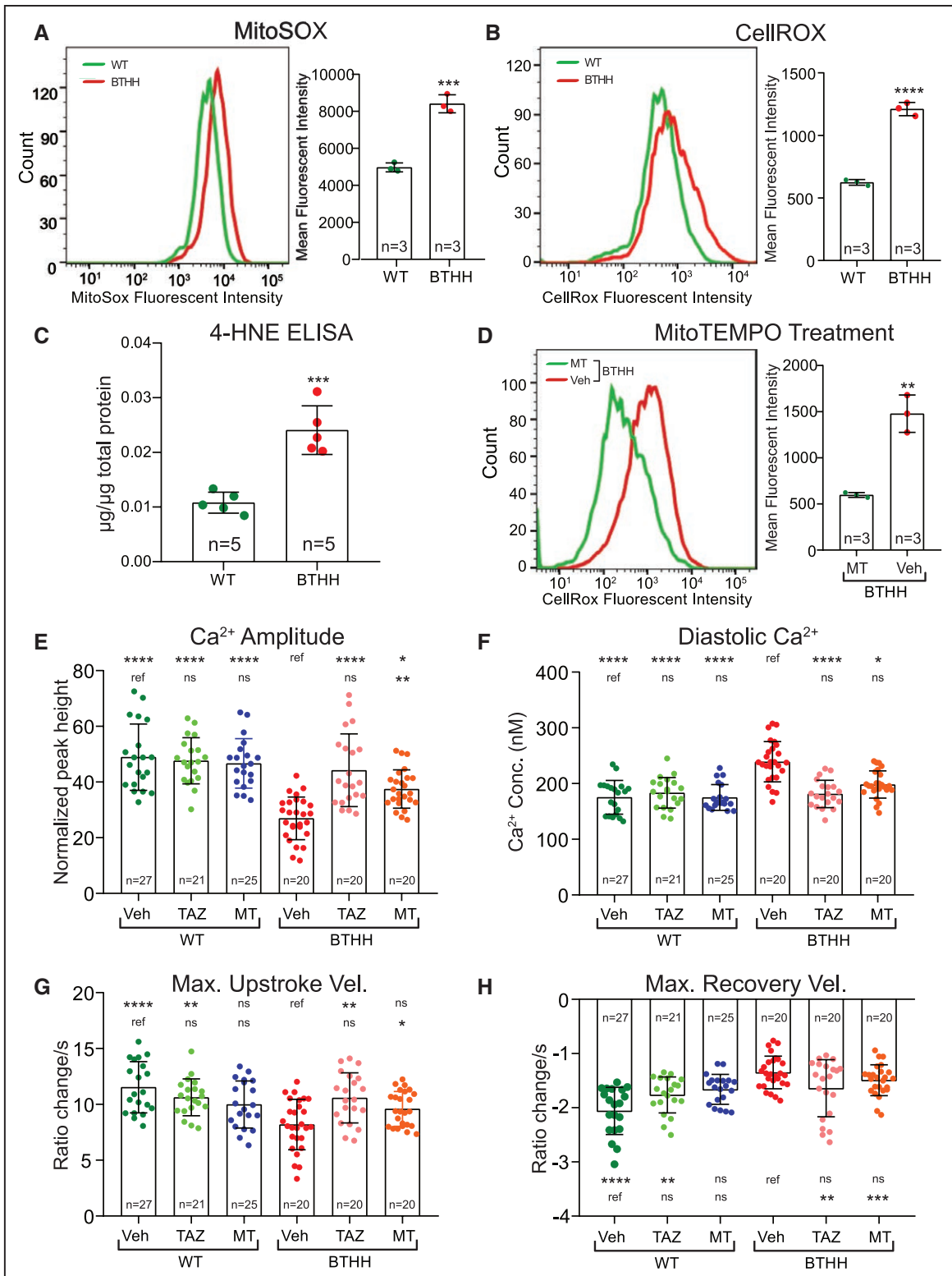
Figure 3. Elevated ROS in *TAZ* mutant iPSC-CMs contributes to abnormal Ca²⁺ handling.
A and **B**, Mitochondrial or cellular ROS levels in BTHH and WT iPSC-CMs were measured by flow cytometry of mitochondria stained with MitoSOX (**A**) or cells stained with CellROX (**B**), respectively. **C**, Levels of the lipid peroxidation product 4-HNE were detected in BTHH and WT iPSC-CMs by ELISA. **D**, MitoTEMPO (MT) treatment reduced ROS levels in BTHH iPSC-CMs to WT levels. **E** through **H**, Effect of MT or *TAZ* modRNA on BTHH iPSC-CM Ca²⁺ handling. Fura-2–loaded iPSC-CMs were electrically paced at 1 Hz and analyzed by ratiometric Ca²⁺ imaging. Comparisons were with either mock-treated BTHH or mock-treated WT, as indicated by the labeled reference (ref.), using Kruskal–Wallis with Dunn multiple comparison test. *$P<0.05$, **$P<0.01$, ***$P<0.001$, ****$P<0.0001$. BTHH indicates Barth syndrome; iPSC-CM, induced pluripotent stem cell–derived cardiomyocyte; ns, not significant; ROS, reactive oxygen species; TAZ, tafazzin; and WT, wild type.

Excessive ROS-Induced CaMKII Activation Leads to Abnormal Ca²⁺ Handling in BTHH iPSC-CMs

CaMKII is a key kinase that modulates the activity of multiple Ca²⁺ handling proteins, including RYR2.[29,30] After activation by calcified calmodulin, CaMKII oxidation or autophosphorylation locks CaMKII in an active form.[30,31] We hypothesized that elevated ROS activates CaMKII in BTHH iPSC-CMs and contributes to their Ca²⁺ handling abnormalities. To test this hypothesis, we measured CaMKII activation in BTHH and control iPSC-CMs using antibodies that detect phosphorylated, activated CaMKII (phosphorylated threonine 286; p-CaMKII), oxidized CaMKII (M281-M282 oxidation; ox-CaMKII), or total CaMKII. Capillary Westerns showed that the ratio of p-CaMKII to total CaMKII (Figure 4A) was significantly higher in BTHH iPSC-CMs. Furthermore, ox-CaMKII–specific antibody demonstrated greater CaMKII oxidation in BTHH iPSC-CMs (Figure 4B and Figure VA in the Data Supplement). To further assess CaMKII activity, we measured PLN (phospholamban) phosphorylation at Thr-17 (p-PLN), a well-established CaMKII phosphorylation site.[32] We observed that p-PLN (PLN monomer) was markedly elevated in BTHH iPSC-CMs (Figure VB in the Data Supplement), consistent with elevated CaMKII activity. Next, we assessed the effect of scavenging ROS by MitoTEMPO treatment on CaMKII activation in BTHH iPSC-CMs. Capillary Westerns showed that MitoTEMPO treatment reduced ox-CaMKII levels in BTHH iPSC-CMs (Figure VC and VD in the Data Supplement). The mean level of p-CaMKII was also lower in MitoTEMPO-treated BTHH iPSC-CMs, but this did not reach statistical significance because of substantial intragroup variation (Figure VC and VD in the Data Supplement). Collectively, these data demonstrate that BTHH iPSC-CMs have elevated levels of activated forms of CaMKII (ox-CaMKII and p-CaMKII) and increased CaMKII activity, as reflected by greater p-PLN, and that CaMKII activation depends on increased mitochondrial ROS.

To evaluate the contribution of increased CaMKII activation to the Ca²⁺ handling abnormalities of BTHH iPSC-CMs, we treated iPSC-CMs with a cell-permeable (myristoylated) form of autocamtide-2-related inhibitory peptide (AIP), a highly potent and selective CaMKII inhibitory peptide,[33] and measured the effect on Ca²⁺ handling. AIP significantly but incompletely corrected BTHH iPSC-CM Ca²⁺ transient amplitude and reduced diastolic Ca²⁺ concentration to a level that was comparable to control (Figure 4C and 4D). Maximal Ca²⁺ transient upstroke velocity of AIP-treated cells had an intermediate value such that it did not significantly differ from either control or BTHH iPSC-CMs (Figure 4E). Maximum Ca²⁺ transient recovery velocity was not

significantly affected by AIP (Figure 4F). AIP treatment of BTHH iPSC-CMs also reduced the aberrant spontaneous Ca²⁺ release observed during or immediately after pacing (Figure IVE and IVF in the Data Supplement). Incomplete correction of Ca²⁺ transient amplitude and upstroke and recovery velocities may have been attributed to incomplete inhibition of CaMKII or to a combination of both CaMKII-dependent and -independent mechanisms that are responsible for the Ca²⁺ handling defects in *TAZ* mutant iPSC-CMs. Indeed, a previous study found that murine TAZ-deficient cardiomyocytes had reduced maximal SERCA2a activity linked to increased tyrosine nitration.[34] Consistent with this study, SERCA2a tyrosine nitration in BTHH iPSC-CMs tended to be higher than in WT ($P=0.09$; Figure VE–VG in the Data Supplement). Other studies have demonstrated that elevated ROS can oxidize RYR2 and thereby increase aberrant Ca²⁺ release. To investigate whether this occurs in BTHH iPSC-CMs, we measured RYR2 oxidation using the monobromobimane assay (Figure VH and VI in the Data Supplement). We did not detect a measurable difference in RYR2 oxidation between control and BTHH iPSC-CMs.

These data implicate mitochondrial ROS activation of CaMKII in the aberrant Ca²⁺ handling of TAZ-deficient iPSC-CMs. Other mechanisms, such as SERCA2a nitration, likely also contribute to the Ca²⁺ handling phenotype.

RYR2 Phosphorylation by CaMKII Contributes to Abnormal Ca²⁺ Handling in *TAZ* Mutant iPSC-CMs

Among the Ca²⁺ handling proteins phosphorylated by CaMKII is RYR2. CaMKII-mediated RYR2 phosphorylation at serine 2814 (RYR2-pS2814) increases RYR2 diastolic Ca²⁺ leak, promotes arrhythmia, and adversely impacts myocardial outcome in heart disease models.[35,36] Our data indicate elevated diastolic Ca²⁺ concentration in conjunction with elevated RYR2 Ca²⁺ flux (Figure 3F and Figure IVA and IVB in the Data Supplement) and ROS-dependent CaMKII activation in BTHH iPSC-CMs. These findings led us to evaluate the contribution of CaMKII-mediated RYR2 at serine 2814[29] to abnormal Ca²⁺ handling in BTHH iPSC-CMs. RYR2-pS2814 immunoreactivity was markedly elevated in BTHH iPSC-CMs, whereas total RYR2 expression levels detected by ELISA were unchanged (Figure 5A).

To delineate the contribution of elevated RYR2-pS2814 to Ca²⁺ handling abnormalities of BTHH iPSC-CMs, we used Cas9 genome editing to ablate this phosphosite by converting serine 2814 to alanine in both *RYR2* alleles in the context of WT or mutant *TAZ*. We confirmed successful genome editing in the WT-S2814A and BTHH-S2814A iPSC lines by Sanger
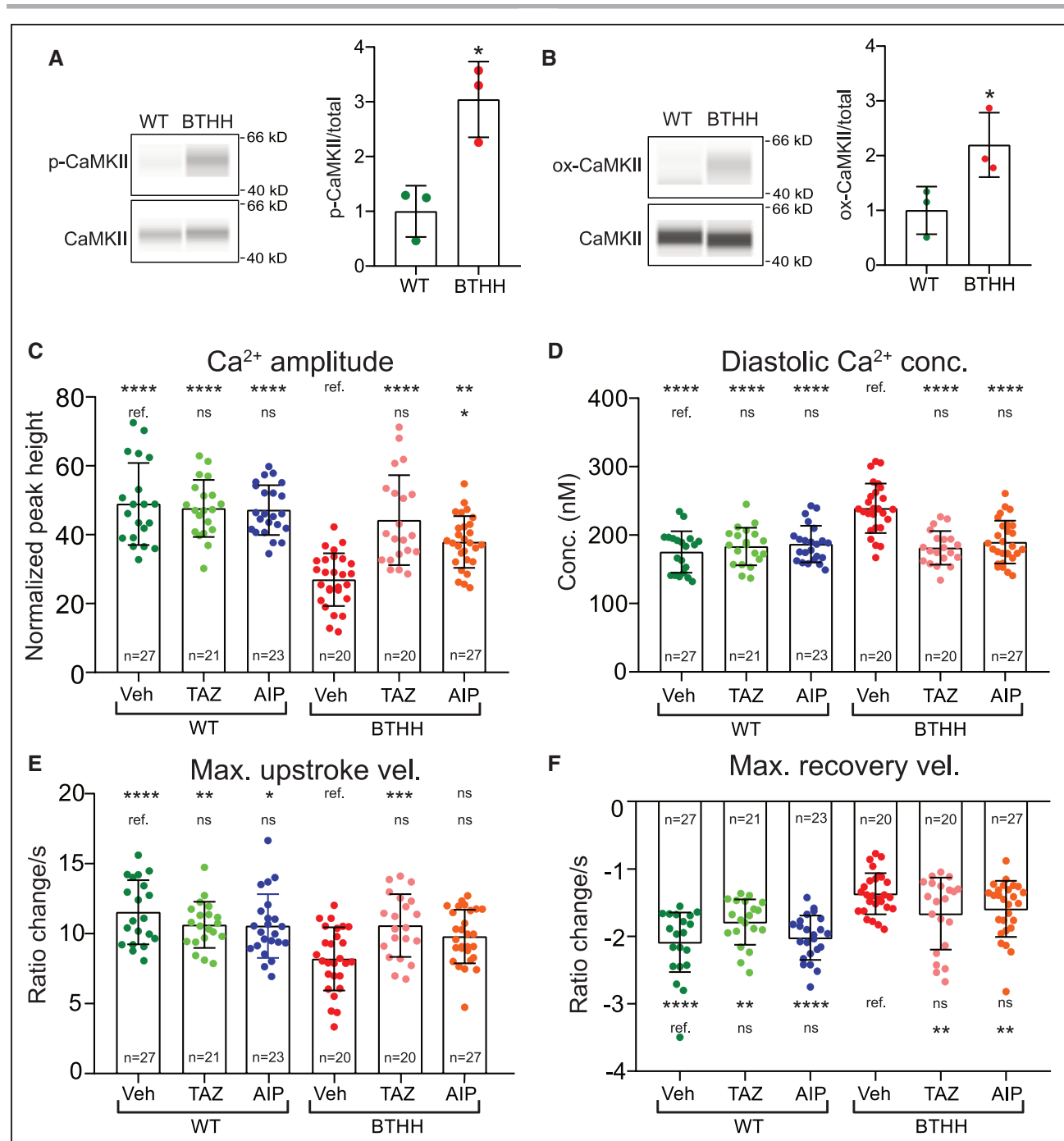
Figure 4. CaMKII activation promotes aberrant Ca²⁺ handling in *TAZ* mutant iPSC-CMs.
A and **B.** Capillary Westerns for phosphorylated (Thr286), oxidized (M281/M282), and total CaMKII, in WT and BTHH iPSC-CMs. **Left**, Representative virtual blot images. **Right**, quantification; *t* test. **C** through **F**, Effect of CaMKII inhibition on BTHH iPSC-CM Ca²⁺ handling. Fura-2–loaded iPSC-CMs were electrically paced at 1 Hz and analyzed by ratiometric Ca²⁺ imaging. Data for vehicle and *TAZ* modRNA groups, statistical analysis, and symbols are the same as in Figure 3E through 3H. BTHH indicates Barth syndrome; CaMKII, Ca²⁺/calmodulin-dependent protein kinase II; iPSC-CM, induced pluripotent stem cell–derived cardiomyocyte; TAZ, tafazzin; WT, wild type.

sequencing of the target loci (Figure 5B). We did not detect off-target genome modification (Table III in the Data Supplement). Immunoblotting confirmed loss of RYR2-S2814 phosphorylation (Figure 5C).

We used ratiometric Ca²⁺ imaging to measure Ca²⁺ transients in BTHH-S2814A and WT-S2814A. In cells with functional TAZ, S2814 mutation did

not significantly affect Ca²⁺ handling (Figure 5D–5G; Figure IVG in the Data Supplement). In contrast, in cells with mutant *TAZ*, ablation of the RYR2-S2814 phosphorylation site increased maximal Ca²⁺ transient upstroke velocity and reduced diastolic Ca²⁺ concentration (Figure 5D–5F). RYR2-S2814A mutation also reduced Ca²⁺ spark frequency of *TAZ* mutant
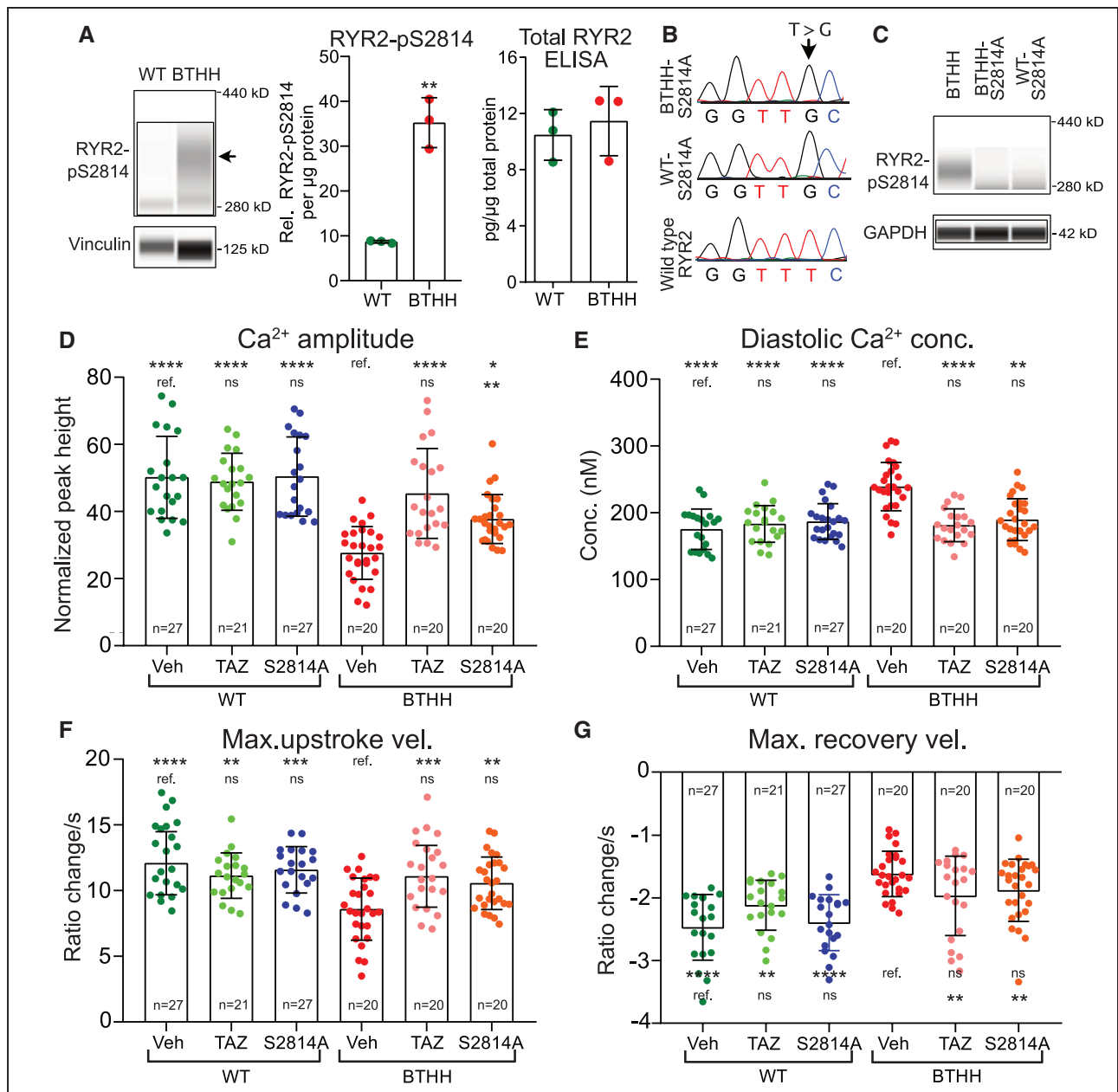
Figure 5. RYR2 phosphorylation contributes to abnormal Ca²⁺ handling in *TAZ* mutant iPSC-CMs.
A. Elevated RYR2-pS2814 in BTHH iPSC-CMs. The level of RYR2 phosphorylated at S2814 was measured by capillary Western. **Left**, Representative virtual image. →, RYR2-pS2814 band. **Middle**, Quantitative analysis of RYR2-pS2814 in BTHH and WT. **Right**, Measurement of total RYR2 by ELISA. Two-tailed *t* test. **B**. Homozygous mutation of RYR2 to convert S2814 to alanine. Dox-induced Cas9 genome editing was used to ablate the RYR2 S2814 phosphosites. Sanger sequencing of a genomic DNA amplicon confirmed successful mutation of both RYR2 alleles in WT and BTHH iPSCs. **C**, Loss of RYR2-S2814 phosphorylation in WT/BTHH-S2814A iPSC-CMs was confirmed by immunoblotting. BTHH iPSC-CMs were used as a positive control. **D** through **G**, Effect of RYR2 S2814A mutation on BTHH and WT Ca²⁺ handling. Fura-2–loaded iPSC-CMs were electrically paced at 1 Hz and analyzed by ratiometric Ca²⁺ imaging. Data for vehicle and *TAZ* modRNA groups, statistical analysis, and symbols are the same as in Figure 3E through 3H. BTHH indicates Barth syndrome; iPSC-CM, induced pluripotent stem cell–derived cardiomyocyte; RYR2, ryanodine receptor 2; and TAZ, tafazzin.

iPSC-CMs (Figure IVG in the Data Supplement). Indeed, diastolic Ca²⁺ concentration and maximal Ca²⁺ transient upstroke velocity became indistinguishable from control cells, suggesting that CaMKII-mediated phosphorylation of RYR2-S2814 plays a predominant role in the derangement of these parameters in *TAZ* mutant cells. However, Ca²⁺ transient amplitude and Ca²⁺ spark frequency were incompletely corrected,

and Ca²⁺ transient recovery velocity was not significantly changed (Figure 5G), suggesting that additional CaMKII targets, or CaMKII-independent mechanisms, contribute to these abnormalities.

Collectively, these results indicate that ROS-mediated CaMKII activation, RYR2-S2814 phosphorylation, and elevated diastolic RYR2 Ca²⁺ flux contribute to abnormal Ca²⁺ handling in BTHH iPSC-CMs.

Activated ROS-CaMKII-RYR2 Pathway Induced Ca²⁺ Abnormalities in *Taz* Mutant Murine Cardiomyocytes

The immaturity of iPSC-CMs can raise questions as to the extent to which observed abnormalities translate to bona fide cardiomyocytes. Therefore, to complement the human iPSC-CMs studies, we studied cardiomyocytes isolated from *Taz^flox* mice, in which loxP elements flank exons 5 to 10.

We first studied ventricular cardiomyocytes prepared from *Taz^flox/Y* (male) neonatal mice. We treated isolated neonatal murine ventricular cardiomyocytes (NMVMs) prepared from these mice with adenovirus that expressed either Cre (Ad:Cre; *Taz* ablated) or LacZ (Ad:LacZ; control). Capillary Western confirmed efficient *Taz* ablation after treatment with Ad:Cre at a multiplicity of infection of 20 (Figure VIA in the Data Supplement). Ad:Cre-treated NMVMs had higher levels of ROS than Ad:LacZ controls (Figure 6A). As in BTHH iPSC-CMs, Ad:Cre-treated NMVMs showed significantly higher levels of ox-CaMKII (Figure VIB and VIC in the Data Supplement). However, the level of p-CaMKII did not differ significantly from controls (Figure VIB and VIC in the Data Supplement). RYR2-pS2814 was markedly elevated and total RYR2 was not significantly altered in *Taz*-deficient NMVMs compared with controls (Figure 6B). These data support ROS-mediated CaMKII activation and RYR2-pS2814 phosphorylation in *Taz* mutant NMVMs.

To evaluate Ca²⁺ handling in *Taz* mutant and control NMVMs, we performed ratiometric Ca²⁺ imaging (Figure 6C–6F; Figure VID in the Data Supplement). Consistent with our observations in *TAZ* mutant iPSC-CMs, *Taz*-ablated NMVMs had significantly lower Ca²⁺ transient amplitude and reduced maximal Ca²⁺ transient upstroke velocity (Figure 6C and 6E). Diastolic Ca²⁺ concentration also tended to be elevated in *Taz* mutant NMVMs (*P*=0.051; Figure 6D). However, unlike the iPSC-CM model, maximal Ca²⁺ transient recovery velocity was not significantly changed in *Taz* mutant NMVMs (Figure 6F). Thus, *Taz* mutant NMVMs exhibited abnormal Ca²⁺ handling that was largely consistent with the abnormalities observed in BTHH iPSC-CMs.

We next evaluated the effect of reducing ROS levels with MitoTEMPO or inhibiting CaMKII with AIP on Ca²⁺ handling of control and *Taz* mutant NMVMs. Consistent with the results from iPSC-CMs, both MitoTEMPO and AIP corrected the Ca²⁺ transient amplitude, diastolic Ca²⁺ concentration, and maximal Ca²⁺ transient upstroke velocity of *Taz* mutant NMVMs so they became indistinguishable from control values (Figure 6C–6F). These results mechanistically implicate mitochondrial ROS and CaMKII activation in the aberrant Ca²⁺ handling of *Taz* mutant NMVMs.

Ca²⁺ handling of cardiomyocytes changes substantially during the first weeks of postnatal life. Therefore we also studied the Ca²⁺ handling of *Taz* mutant (*Myh6Cre⁺; Taz^fl/Y*) and control (*Myh6Cre⁻;Taz^fl/Y*) adult murine ventricular cardiomyocytes (AMVMs). Using both CellRox staining and ELISA to measure levels of the lipid peroxidation product 4-HNE, we confirmed elevated levels of ROS in *Taz* mutant AMVMs (Figure 7A; Figure VIE in the Data Supplement). By capillary Western, ox-CaMKII tended to be elevated in *Taz* mutant AMVMs (*P*=0.077; Figure VIF and VIG in the Data Supplement). Mean p-CaMKII:total CaMKII ratio was elevated in *Taz* mutant AMVMs, although this observation did not reach statistical significance (Figure VIF and VIG in the Data Supplement). *Taz* mutant AMVMs also had significantly elevated phosphorylation of CaMKII targets RYR2-pS2814 (Figure 7B) and PLN-pT17 (Figure VIH in the Data Supplement).

Ratiometric Ca²⁺ imaging demonstrated that the *Taz* mutant AMVMs had Ca²⁺ handling defects similar to those observed in iPSC-CMs (Figure 7C–7F; Figure VID in the Data Supplement): reduced Ca²⁺ transient amplitude, elevated diastolic Ca²⁺ concentration, and lower maximal Ca²⁺ transient recovery velocity. However, Ca²⁺ transient maximal upstroke velocity was not significantly altered. Inhibition of CaMKII by AIP tended to increase the Ca²⁺ transient amplitude (*P*=0.058; Figure 7C) and significantly reduced the diastolic Ca²⁺ concentration (Figure 7D). However, AIP treatment of *Taz* mutant AMVMs did not significantly correct the maximal Ca²⁺ transient recovery velocity and did not significantly affect the maximal Ca²⁺ upstroke velocity (Figure 7E and 7F).

Together these data demonstrate that *Taz* mutant, bona fide murine cardiomyocytes have Ca²⁺ handling abnormalities that are largely consistent with those observed in iPSC-CMs and that are ameliorated by reduction of ROS or inhibition of CaMKII.

Normalization of Ca²⁺ Handling Improves BTHH EHT Contractile Function

Ca²⁺ is the central mediator of excitation-contraction coupling. Reduced Ca²⁺ transient amplitude and Ca²⁺ upstroke velocity, as well as elevated diastolic Ca²⁺, impair cardiomyocyte contraction and relaxation, respectively. To investigate a potential link between aberrant Ca²⁺ handling and contractile dysfunction in BTHS, we assembled control or BTHH iPSC-CMs, transduced with the optogenetic actuator ChR2-YFP, into EHTs (Figure VIIA in the Data Supplement). BTHH iPSC-CMs cultured on a stiff, 2-dimensional, patterned substrate exhibited defective sarcomere organization.[10] In the 3-dimensional EHT context, both control and BTHH iPSC-CMs displayed elongated, aligned morphology and well-organized sarcomeres
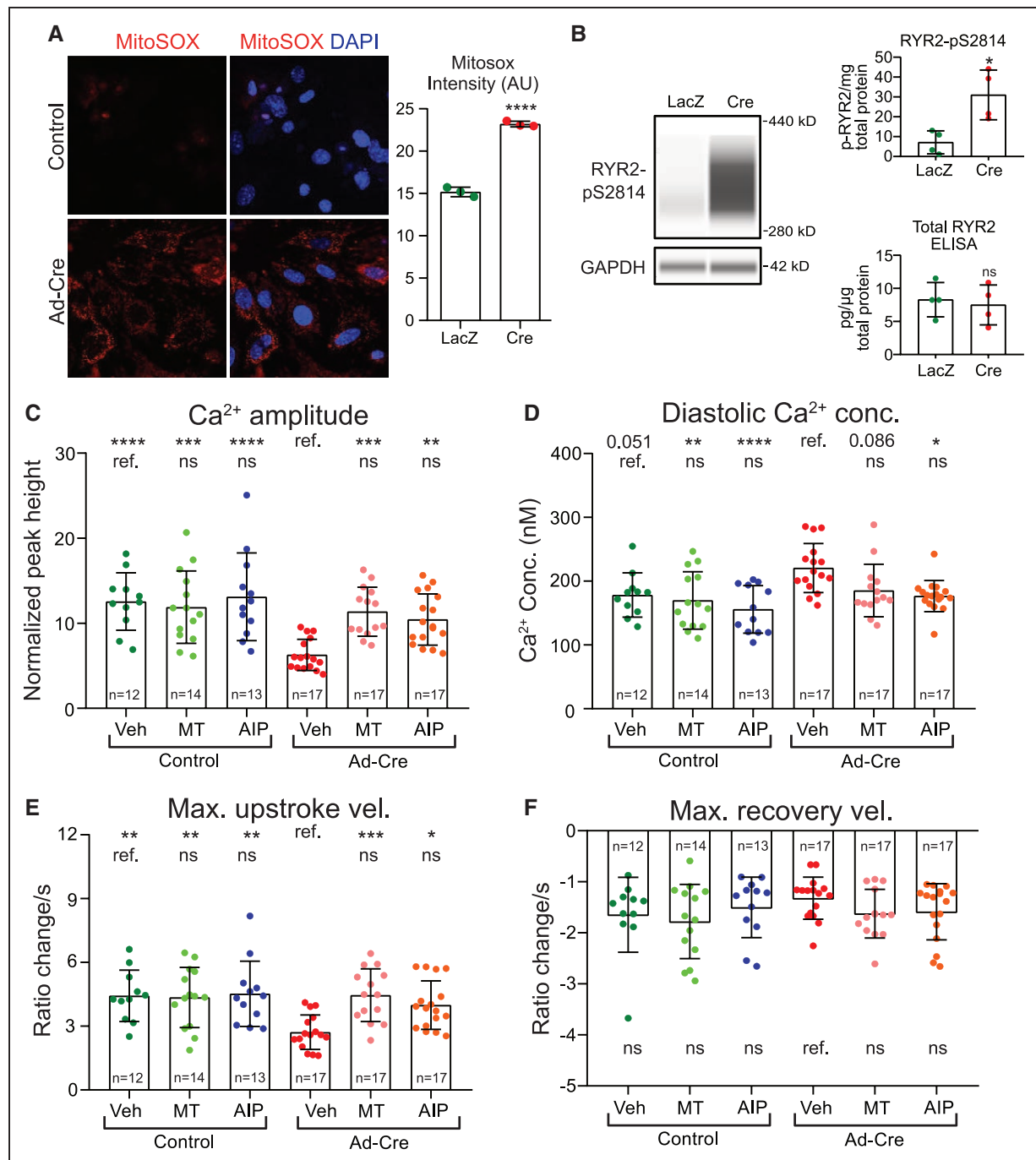
Figure 6. Abnormal Ca²⁺ handling in Taz KO neonatal mouse ventricular cardiomyocytes.
A, Mitochondrial ROS levels in control and *Taz*-ablated neonatal mouse ventricular cardiomyocytes. Cultured *Tazfl/fl* neonatal mouse ventricular cardiomyocytes were treated with Ad-Cre or Ad-LacZ. Three days later they were stained with MitoSox and DAPI. **Left**, Representative image. **Right**, Quantitative analysis of the mean fluorescence intensity of 3 randomly acquired fields per group. Two-tailed *t* test. **B**, RYR2-S2814 phosphorylation in *Taz* mutant or control NMVMs. **Left**, Representative virtual capillary Western image. **Top right**, Quantification of capillary Western measurement of RYR2-pS2814. **Bottom right**, ELISA quantification of total RYR2 level. Two-tailed *t* test. **C** through **F**, Effect of ROS scavenger (MT) or CaMKII inhibition (AIP) on Ca²⁺ transients in *Taz* KO and control NMVMs. Fura-2–loaded NMVMs were electrically paced at 1 Hz and analyzed by ratiometric Ca²⁺ imaging. Only Ca²⁺ transient amplitude fit a normal distribution and was analyzed by ANOVA with the Dunnett multiple comparison test, whereas the remaining parameters were analyzed by Kruskal–Wallis with Dunn multiple comparison test. Comparisons were to either mock-treated *Taz* KO or mock-treated WT, as indicated by the labeled reference (ref.) group in each row. *P<0.05, **P<0.01, ***P<0.001, ****P<0.0001. AIP indicates autocamtide-2-related inhibitory peptide; KO, knockout; MT, MitoTEMPO; NMVM, neonatal murine ventricular cardiomyocyte; ns, not significant; ROS, reactive oxygen species; RYR2, ryanodine receptor 2; and TAZ, tafazzin.

(Figure VIIB and VIIC in the Data Supplement), indicating that the EHT culture conditions enabled cells to overcome barriers to sarcomere assembly posed by TAZ deficiency in the cell patterning assay.[10] Nevertheless, BTHH EHTs showed weaker contraction than controls (3.7-fold reduction; Figure 8A; Video II in the
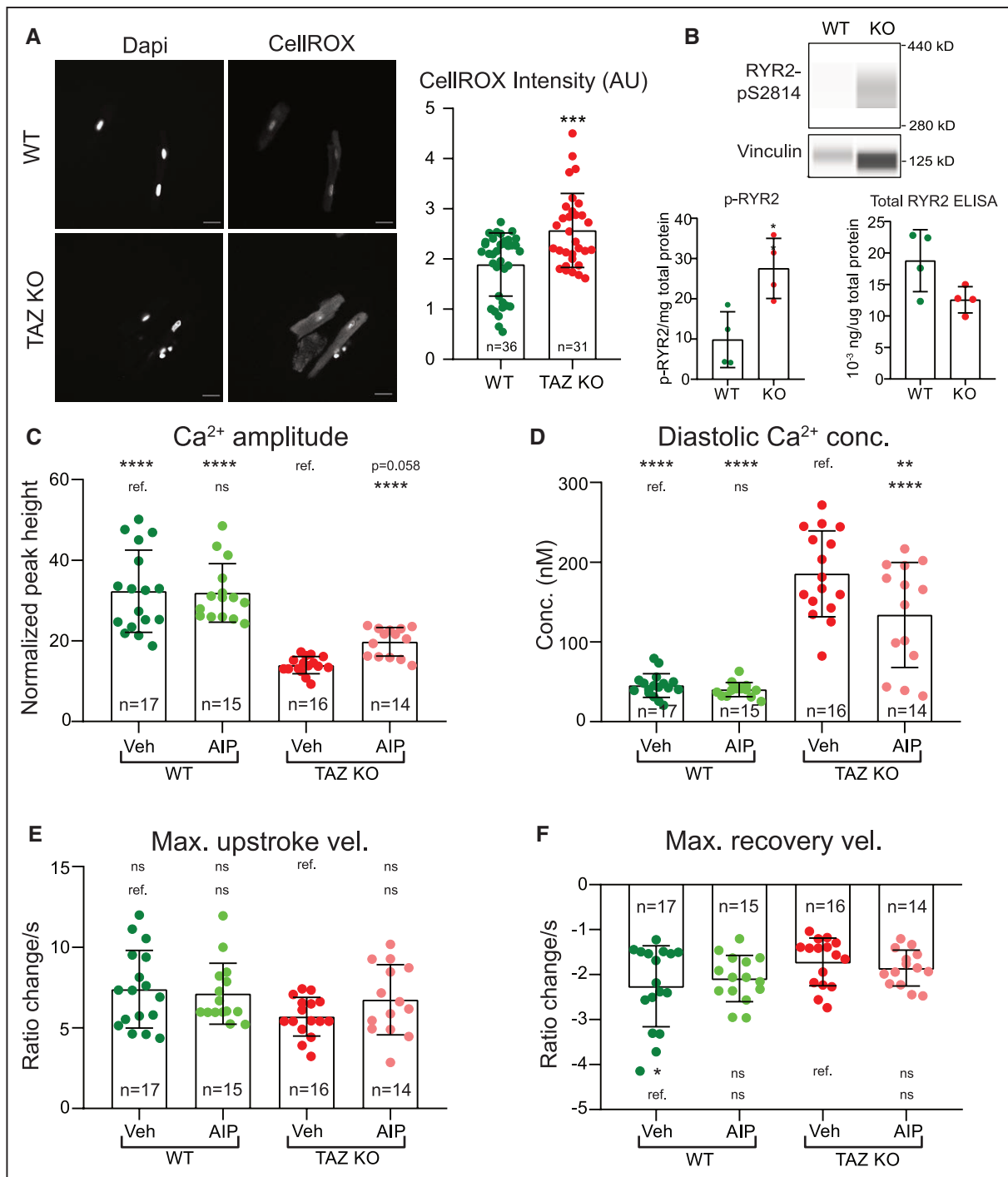
Figure 7. Abnormal Ca²⁺ handling in adult *Taz* KO mice ventricular cardiomyocytes.
A, ROS levels in isolated *Taz* KO and control AMVMs. Cells were stained with CellROX. **Left**, Representative images. **Right**, Quantification. Each point represents 1 cell. Two-tailed *t* test. **B**, RYR2-S2814 phosphorylation in *Taz* KO and control AMVMs. RYR2-pS2814 was measured by capillary Western. **Top**, Capillary Western virtual image. **Bottom left**, RYR2-pS2814 quantification. **Bottom right**, Total RYR2 quantification by ELISA. Two-tailed *t* test. **C** through **F**, Ca²⁺ transient parameters of *Taz* KO and control AMVMs. Two-month-old *Taz* KO (Myh6Cre⁺; TAZ^fl/Y) and control AMVMs were dissociated, loaded with Fura-2, and analyzed using ratiometric Ca²⁺ imaging with 1 Hz pacing and AIP or vehicle treatment. Maximal Ca²⁺ upstroke velocities were analyzed with Kruskal–Wallis with Dunn multiple comparison test, whereas the remaining parameters were analyzed by ANOVA with Dunnett multiple comparison test. Comparisons were with either vehicle-treated *Taz* KO or WT, as indicated by the labeled reference group (ref.) in each row. *$P<0.05$, **$P<0.01$, ***$P<0.001$, ****$P<0.0001$. AIP indicates autocamtide-2-related inhibitory peptide; AMVM, adult murine ventricular cardiomyocytes; KO, knockout; ns, not significant; ROS, reactive oxygen species; RYR2, ryanodine receptor 2; and TAZ, tafazzin.

Data Supplement), consistent with our previous studies of *TAZ* mutant muscular thin films.[10]

We studied the effect of *TAZ* replacement by *TAZ* modRNA, ROS scavenging by MitoTEMPO, and CaMKII

inhibition by AIP on BTHH EHT contraction (Figure 8B). *TAZ* modRNA, MitoTEMPO, and AIP treatments did not alter the contractile function of control EHTs (Figure 8C–8E). In contrast, *TAZ* modRNA markedly improved the
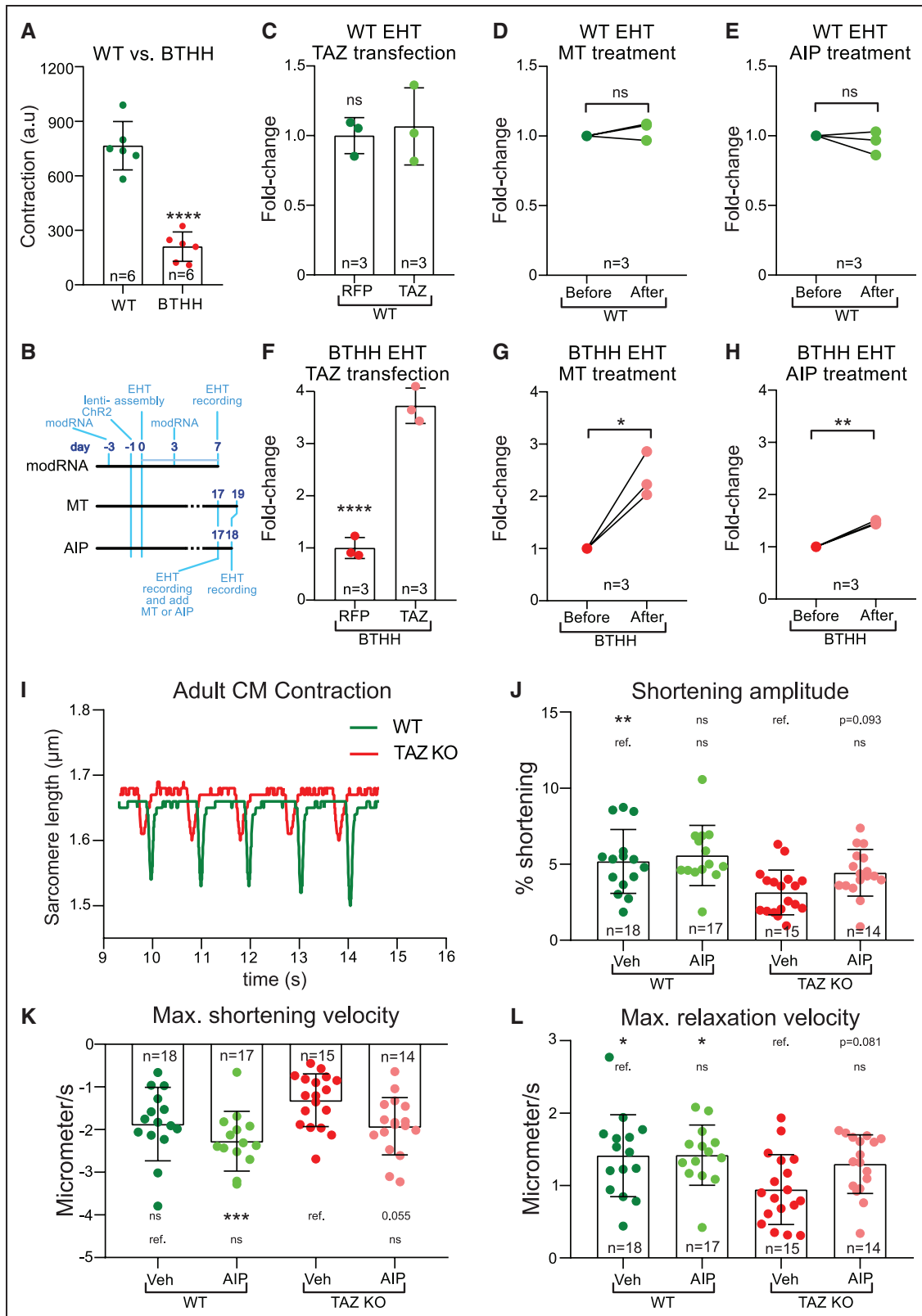
Figure 8. Inhibition of ROS–CaMKII–RYR2 pathway restored contractile function of *TAZ* mutant cardiomyocytes.
A, Reduced contractile function of BTHH EHTs compared with controls. BTHH or control iPSC-CMs were assembled into EHTs. Contractile function was measured at 14 days after EHTs started contracting using MuscleMotion. Two-tailed *t* test. **B** through **H**, Effect of *TAZ* modRNA, MT, or AIP on control or BTHH EHT contractile function. **B**, experimental timelines. *TAZ* or RFP modRNA iPSC-CMs were assembled into EHTs. EHTs were treated again with *TAZ* or RFP modRNA on day 3. EHTs were assayed on day 7. Two-tailed *t* test. For MT or AIP experiments, EHTs were assayed on day 17 before treatment. EHTs were then treated with AIP or MT for 1 or 2 days, respectively, and then assayed again. Relative contractile function is expressed as fold-change compared with pretreatment values. Paired *t* test. **C** and **F**, TAZ modRNA treatment of WT or BTHH EHTs. **D** and **G**, MT treatment of WT or BTHH EHTs. **E** and **H**, AIP treatment of WT or BTHH EHTs. (*Continued*)

Figure 8 Continued. I through **L**, Effect of *TAZ* mutation and CaMKII inhibition on AMVM contractile function. Cardiomyocytes were isolated from 2-month-old *Taz* KO (*Myh6Cre*+; *Taz*^fl/Y^) or control hearts. Contractile function of individual myocytes was measured by video measurement of sarcomere length. **I**, Representative traces of WT and *Taz* KO sarcomere length during 1-Hz pacing. **J**, Fractional shortening of *Taz* KO and control cardiomyocytes treated for 2 hours with vehicle or AIP. **K** and **L**, Maximal velocity of shortening or relaxation of WT and *Taz* KO cardiomyocytes. Maximal shortening velocity did not fit a normal distribution and was analyzed with Kruskal–Wallis with a Dunn multiple comparison test, whereas the remaining parameters were analyzed by ANOVA with a Dunnett multiple comparison test. Comparisons were either mock-treated BTHH or mock-treated WT, as indicated by the labeled reference (ref.) group in each row. *$P<0.05$, **$P<0.01$, ***$P<0.001$, ****$P<0.0001$. AIP indicates autocamtide-2-related inhibitory peptide; AMVM, adult murine ventricular cardiomyocyte; a.u., arbitrary units; BTHH, TAZ mutant line; CaMKII, Ca2+/calmodulin-dependent protein kinase II; EHT, engineered heart tissues; KO, knockout; iPSC-CM, induced pluripotent stem cell–derived cardiomyocyte; modRNA, modified mRNA; MT, MitoTEMPO; ns, not significant; RFP, red fluorescent protein; ROS, reactive oxygen species; RYR2, ryanodine receptor 2; TAZ, tafazzin; and WT, wild type.

contraction of BTHH EHTs by 3.7-fold (Figure 8F; Video III in the Data Supplement), indicating that the contractile defects are largely reversible by gene replacement. Scavenging ROS with MitoTEMPO partially restored contractile function (2.4-fold, Figure 8G; Video IV in the Data Supplement), although not to the same level as *TAZ* modRNA (Figure 8F). Treatment of EHTs with AIP also improved contractile function (1.5-fold; Figure 8H; Video V in the Data Supplement), although the effect was weaker than that of *TAZ* modRNA or MitoTEMPO.

We further evaluated the effect of *TAZ* mutation on AMVM contraction, using edge detection to measure sarcomere length during the contraction of dissociated cardiomyocytes. *TAZ* mutant (*Myh6Cre; Taz*^fl/Y^) and control cardiomyocytes were isolated from 2-month-old mice, when the mutant mice have mild cardiac dysfunction.[27] Consistent with the EHT model, individual *TAZ* mutant cardiomyocytes had reduced contraction amplitude ($P<0.01$) and relaxation velocity ($P<0.05$; Figure 8I–8L). Treatment with AIP to inhibit CaMKII tended to increase contraction amplitude ($P=0.093$), shortening velocity ($P=0.055$) and relaxation velocity ($P=0.081$; Figure 8J–8L). These data suggest that TAZ deficiency contributes to impaired contraction of individual cardiomyocytes and implicate excessive CaMKII activation as a factor in *TAZ* mutant cardiomyocyte dysfunction.

DISCUSSION

Patients with BTHS have cardiomyopathy and risk of sudden cardiac death from incompletely described arrhythmias.[7–9,26] Here we studied mice with cardiac-restricted *Taz* knockout and show that a subset developed complete heart block, atrial tachycardia, and bidirectional VT, which were not observed in WTs. The significance of complete heart block after anesthesia and catheter placement but before drug treatment or ventricular stimulation is uncertain, because some vulnerable mice develop this arrhythmia nonspecifically under anesthesia, and progressive functional heart block has not been reported to our knowledge in patients with BTHS. On the other hand, VT requiring implantable cardioverter defibrillator placement occurs in some patients with BTHS.[7–9,26] A subset of Barth mice developed bidirectional VT under adrenergic stimulation. This arrhythmia is closely associated with dysregulated Ca2+ handling in digitalis toxicity and catecholaminergic

polymorphic VT because of mutations in *RYR2*.[28] In the latter condition, we demonstrated recently that RYR2-S2814 phosphorylation by CaMKII is a critical event that unmasks latent arrhythmia mutations during catecholamine stimulation.[14,22] Our results suggest that, in BTHS, ROS-mediated CaMKII activation drives excessive RYR2-S2814 phosphorylation, predisposing hearts to the development of bidirectional VT. Unfortunately the low penetrance of VT in this model will make it difficult to use for therapeutic trials of antiarrhythmic efficacy.

The mechanisms that lead from *TAZ* mutation to contractile dysfunction and arrhythmia are incompletely understood. Diminished energy reserves may contribute to baseline cardiac dysfunction and limited augmentation of heart function with exercise in patients with BTHS.[37] iPSC-CMs successfully model aspects of the BTHS cardiomyopathy phenotype.[10,38] In iPSC-CMs, the cardiomyopathy phenotype was corrected by normalization of ROS levels with MitoTEMPO but not by culture conditions that normalized ATP levels.[10] Here we demonstrate that elevated ROS in BTHS iPSC-CMs and murine cardiomyocytes activate CaMKII and impair Ca2+ handling, which could contribute to both cardiac dysfunction and arrhythmias.

Oxidative stress is well established to exacerbate cardiac dysfunction and predispose to arrhythmias. A key mediator of these deleterious effects of ROS is CaMKII, which can be "locked" in an activated state by oxidation of methionine 281/282.[30,31] Here, we link mitochondrial ROS production in *TAZ* mutant cardiomyocytes with CaMKII activation. *TAZ* mutation likely elevates mitochondrial ROS through at least 2 mechanisms. First, *TAZ* mutation destabilizes electron transport chain supercomplexes by impairing the biogenesis of cardiolipin, which is required for supercomplex assembly.[38–41] Second, *TAZ* mutation impairs mitophagy, thereby reducing mitochondrial quality control.[42] Extension of excessive ROS into the cytoplasm, likely in the form of hydrogen peroxide, activates CaMKII and exposes the myocardium to its associated deleterious outcomes. The mechanism likely extends to other forms of mitochondrial disease, which trigger increased levels of oxidative stress.

Our identification of a ROS-CaMKII pathway that is active in the pathogenesis of cardiac disease in BTHS suggests that antagonizing this pathway may be a productive therapeutic strategy. In mice with partial *TAZ* depletion induced by short hairpin RNA against *TAZ*,

elevated ROS levels were detected, but expression of mitochondrially targeted catalase did not affect cardiac function.[11] However, these mice did not exhibit cardiac dysfunction and cardiac rhythm was not investigated, so it was not possible to evaluate the contribution of ROS to pathogenesis of this phenotype. CaMKII activation has been implicated in the pathogenesis of multiple forms of heart disease and arrhythmia.[43,44] Our studies suggest that CaMKII inhibition may improve heart function and ameliorate arrhythmia in BTHS and potentially other mitochondrial myopathies with elevated ROS production. However, it is important to note that CaMKII inhibition only partially rescued most phenotypes, possibly from a combination of incomplete inhibition and important contributions of CaMKII-independent mechanisms, including increased tyrosine nitrosylation of SERCA2a. Among potential additional mechanisms are other kinases activated downstream of oxidative stress, including mitogen activated protein kinases, protein kinase A, some protein kinase C isoforms, protein kinase D, and protein kinase G, as well as direct oxidation or nitrosylation of key biomolecules, including sarcomeric proteins such as titin.[45]

Across the iPSC-CM and murine *TAZ* mutant models that we studied, a common feature was elevated diastolic Ca^{2+} concentration. Elevated diastolic Ca^{2+} concentration was associated with increased diastolic Ca^{2+} leak through RYR2 and was fully corrected by suppression of ROS, inhibition of CaMKII, and ablation of the RYR2-S2814 CaMKII phosphosite, which is known to increase RYR2 diastolic Ca^{2+} leak.[36] These data strongly implicate ROS–CaMKII–RYR2-S2814 phosphorylation as a primary mechanism underlying elevation of diastolic Ca^{2+} in *TAZ* mutant cardiomyocytes. Elevated diastolic Ca^{2+} impairs cardiac relaxation[46] and promotes cardiac arrhythmias,[12] phenotypes observed in some patients with BTHS. Additional studies are needed to fully test this hypothesis and to evaluate whether interruption of this signaling pathway can ameliorate these disease phenotypes in BTHS animal models and patients.

In conclusion, our studies identify Ca^{2+} handling abnormalities in both human iPSC-derived and murine cardiomyocytes with *TAZ* mutation. We show that ROS-mediated activation of CaMKII contributes to the pathogenesis of aberrant Ca^{2+} handling in BTHS. These mechanistic insights suggest therapeutic approaches to cardiac dysfunction and arrhythmia in BTHS and possibly other mitochondrial cardiomyopathies. Because cardiolipin abnormalities are also observed in acquired heart disease,[3,4] the mechanisms revealed by this study may also contribute to the pathogenesis of more prevalent forms of heart disease.

ARTICLE INFORMATION

Correspondence

William T. Pu, MD, Department of Cardiology, Boston Children's Hospital, 300 Longwood Ave, Boston, MA 02115. Email william.pu@cardio.chboston.org

Affiliations

Department of Cardiology, Boston Children's Hospital, MA (X.L., S.W., X.G., R.O., F.L., M.P., S.d.l.S.B., Q.M., G.W., J.C., Y.G., V.J.B., W.T.P.). Department of Radiology, Basic Medical School, Chongqing Medical University, China (X.L.). Center of Scientific Research, the Second Affiliated Hospital and Yuying Children's Hospital of Wenzhou Medical University, Zhejiang, China (X.G.). Key Laboratory of Birth Defects and Related Diseases of Women and Children of MOE, Department of Pediatrics, West China Second University Hospital, Sichuan University, Chengdu (Y.L.). State Key Laboratory of Biocatalysis and Enzyme Engineering, School of Life Science, Hubei University, Wuhan, China (D.Z.). Harvard College, Cambridge, MA (J.C.). Department of Cardiology, Massachusetts General Hospital, Boston (L.X., D.J.M.). Department of Anesthesiology, New York University School of Medicine (Y.X., M.S.). Harvard Stem Cell Institute, Cambridge, MA (W.T.P.).

Disclosures

Drs Pu and Bezzerides hold intellectual property on AAV-mediated inhibition of CaMKII for treatment of cardiac arrhythmias and for treatment of Barth syndrome and are conducting research sponsored by Cydan and Sarepta on CaMKII inhibition for the treatment of catecholaminergic polymorphic ventricular tachycardia.

Supplemental Materials

Expanded Methods
Data Supplement Figures I–VII
Data Supplement Tables I–III
Data Supplement Videos I–V
References 47–56

REFERENCES

1. Ren M, Phoon CK, Schlame M. Metabolism and function of mitochondrial cardiolipin. *Prog Lipid Res.* 2014;55:1–16. doi: 10.1016/j.plipres.2014.04.001

2. Raja V, Greenberg ML. The functions of cardiolipin in cellular metabolism-potential modifiers of the Barth syndrome phenotype. *Chem Phys Lipids.* 2014;179:49–56. doi: 10.1016/j.chemphyslip.2013.12.009

3. Sabbah HN. Targeting the mitochondria in heart failure: a translational perspective. *JACC: Basic to Translational Science.* 2020;5:88–106.

4. Chicco AJ, Sparagna GC. Role of cardiolipin alterations in mitochondrial dysfunction and disease. *Am J Physiol Cell Physiol.* 2007;292:C33–C44. doi: 10.1152/ajpcell.00243.2006

5. Bione S, D'Adamo P, Maestrini E, Gedeon AK, Bolhuis PA, Toniolo D. A novel X-linked gene, G4.5. is responsible for Barth syndrome. *Nat Genet.* 1996;12:385–389. doi: 10.1038/ng0496-385

6. Saric A, Andreau K, Armand AS, Møller IM, Petit PX. Barth syndrome: from mitochondrial dysfunctions associated with aberrant production of reactive oxygen species to pluripotent stem cell studies. *Front Genet.* 2015;6:359. doi: 10.3389/fgene.2015.00359

7. Clarke SL, Bowron A, Gonzalez IL, Groves SJ, Newbury-Ecob R, Clayton N, Martin RP, Tsai-Goodman B, Garratt V, Ashworth M, et al. Barth syndrome. *Orphanet J Rare Dis.* 2013;8:23. doi: 10.1186/1750-1172-8-23

8. Roberts AE, Nixon C, Steward CG, Gauvreau K, Maisenbacher M, Fletcher M, Geva J, Byrne BJ, Spencer CT. The Barth Syndrome Registry: distinguishing disease characteristics and growth data from a longitudinal study. *Am J Med. Genet A.* 2012;158A:2726–2732. doi: 10.1002/ajmg.a.35609

9. Spencer CT, Bryant RM, Day J, Gonzalez IL, Colan SD, Thompson WR, Berthy J, Redfearn SP, Byrne BJ. Cardiac and clinical phenotype in Barth syndrome. *Pediatrics.* 2006;118:e337–e346. doi: 10.1542/peds.2005-2667

10. Wang G, McCain ML, Yang L, He A, Pasqualini FS, Agarwal A, Yuan H, Jiang D, Zhang D, Zangi L, et al. Modeling the mitochondrial cardiomyopathy of Barth syndrome with induced pluripotent stem cell and heart-on-chip technologies. *Nat Med.* 2014;20:616–623. doi: 10.1038/nm.3545

11. Johnson JM, Ferrara PJ, Verkerke ARP, Coleman CB, Wentzler EJ, Neufer PD, Kew KA, de Castro Brás LE, Funai K. Targeted overexpression of catalase to mitochondria does not prevent cardioskeletal myopathy in Barth syndrome. *J Mol Cell Cardiol.* 2018;121:94–102. doi: 10.1016/j.yjmcc.2018.07.001

12. Landstrom AP, Dobrev D, Wehrens XHT. Calcium signaling and cardiac arrhythmias. *Circ Res.* 2017;120:1969–1993. doi: 10.1161/CIRCRESAHA.117.310083

13. Wang G, Yang L, Grishin D, Rios X, Ye LY, Hu Y, Li K, Zhang D, Church GM, Pu WT. Efficient, footprint-free human iPSC genome editing by consolidation of Cas9/CRISPR and piggyBac technologies. *Nat Protoc.* 2017;12:88–103. doi: 10.1038/nprot.2016.152

14. Park SJ, Zhang D, Qi Y, Li Y, Lee KY, Bezzerides VJ, Yang P, Xia S, Kim SL, Liu X, et al. Insights into the pathogenesis of catecholaminergic polymorphic ventricular tachycardia from engineered human heart tissue. *Circulation.* 2019;140:390–404. doi: 10.1161/CIRCULATIONAHA.119.039711

15. Lian X, Hsiao C, Wilson G, Zhu K, Hazeltine LB, Azarin SM, Raval KK, Zhang J, Kamp TJ, Palecek SP. Robust cardiomyocyte differentiation from human pluripotent stem cells via temporal modulation of canonical Wnt signaling. *Proc Natl Acad Sci U S A.* 2012;109:E1848–E1857. doi: 10.1073/pnas.1200250109

16. Lian X, Zhang J, Azarin SM, Zhu K, Hazeltine LB, Bao X, Hsiao C, Kamp TJ, Palecek SP. Directed cardiomyocyte differentiation from human pluripotent stem cells by modulating Wnt/β-catenin signaling under fully defined conditions. *Nat Protoc.* 2013;8:162–175. doi: 10.1038/nprot.2012.150

17. Shannon TR, Ginsburg KS, Bers DM. Quantitative assessment of the SR Ca2+ leak-load relationship. *Circ Res.* 2002;91:594–600. doi: 10.1161/01.res.0000036914.12686.28

18. Shang W, Lu F, Sun T, Xu J, Li LL, Wang Y, Wang G, Chen L, Wang X, Cannell MB, et al. Imaging Ca2+ nanosparks in heart with a new targeted biosensor. *Circ Res.* 2014;114:412–420. doi: 10.1161/CIRCRESAHA.114.302938

19. Addis RC, Ifkovits JL, Pinto F, Kellam LD, Esteso P, Rentschler S, Christoforou N, Epstein JA, Gearhart JD. Optimization of direct fibroblast reprogramming to cardiomyocytes using calcium activity as a functional measure of success. *J Mol Cell Cardiol.* 2013;60:97–106. doi: 10.1016/j.yjmcc.2013.04.004

20. Breckwoldt K, Letuffe-Brenière D, Mannhardt I, Schulze T, Ulmer B, Werner T, Benzin A, Klampe B, Reinsch MC, Laufer S, et al. Differentiation of cardiomyocytes and generation of human engineered heart tissue. *Nat Protoc.* 2017;12:1177–1197. doi: 10.1038/nprot.2017.033

21. Sala L, van Meer BJ, Tertoolen LGJ, Bakkers J, Bellin M, Davis RP, Denning C, Dieben MAE, Eschenhagen T, Giacomelli E, et al. MUSCLEMOTION: a versatile open software tool to quantify cardiomyocyte and cardiac muscle contraction in vitro and in vivo. *Circ Res.* 2018;122:e5–e16. doi: 10.1161/CIRCRESAHA.117.312067

22. Bezzerides VJ, Caballero A, Wang S, Ai Y, Hylind RJ, Lu F, Heims-Waldron DA, Chambers KD, Zhang D, Abrams DJ, Pu WT. Gene therapy for catecholaminergic polymorphic ventricular tachycardia by inhibition of Ca2+/calmodulin-dependent kinase II. *Circulation.* 2019;140:405–419. doi: 10.1161/CIRCULATIONAHA.118.038514

23. Ren M, Xu Y, Erdjument-Bromage H, Donelian A, Phoon CKL, Terada N, Strathdee D, Neubert TA, Schlame M. Extramitochondrial cardiolipin suggests a novel function of mitochondria in spermatogenesis. *J Cell Biol.* 2019;218:1491–1502. doi: 10.1083/jcb.201808131

24. Lin Z, Zhou P, von Gise A, Gu F, Ma Q, Chen J, Guo H, van Gorp PR, Wang DZ, Pu WT. Pi3kcb links Hippo-YAP and PI3K-AKT signaling pathways to promote cardiomyocyte proliferation and survival. *Circ Res.* 2015;116:35–45. doi: 10.1161/CIRCRESAHA.115.304457

25. Li D, Wu J, Bai Y, Zhao X, Liu L. Isolation and culture of adult mouse cardiomyocytes for cell signaling and in vitro cardiac hypertrophy. *J Vis Exp.* 2014;87:51357. doi: 10.3791/51357

26. Spencer CT, Byrne BJ, Gewitz MH, Wechsler SB, Kao AC, Gerstenfeld EP, Merliss AD, Carboni MP, Bryant RM. Ventricular arrhythmia in the X-linked cardiomyopathy Barth syndrome. *Pediatr Cardiol.* 2005;26:632–637. doi: 10.1007/s00246-005-0873-z

27. Wang S, Li Y, Xu Y, Ma Q, Lin Z, Schlame M, Bezzerides VJ, Strathdee D, Pu WT. AAV gene therapy prevents and reverses heart failure in a murine knockout model of Barth syndrome. *Circ Res.* 2020;126:1024–1039. doi: 10.1161/CIRCRESAHA.119.315956

28. Leenhardt A, Denjoy I, Guicheney P. Catecholaminergic polymorphic ventricular tachycardia. *Circ Arrhythm Electrophysiol.* 2012;5:1044–1052. doi: 10.1161/CIRCEP.111.962027

29. Wehrens XH, Lehnart SE, Reiken SR, Marks AR. Ca2+/calmodulin-dependent protein kinase II phosphorylation regulates the cardiac ryanodine receptor. *Circ Res.* 2004;94:e61–e70. doi: 10.1161/01.RES.0000125626.33738.E2

30. Erickson JR, He BJ, Grumbach IM, Anderson ME. CaMKII in the cardiovascular system: sensing redox states. *Physiol Rev.* 2011;91:889–915. doi: 10.1152/physrev.00018.2010

31. Erickson JR, Joiner ML, Guan X, Kutschke W, Yang J, Oddis CV, Bartlett RK, Lowe JS, O'Donnell SE, Aykin-Burns N, et al. A dynamic pathway for calcium-independent activation of CaMKII by methionine oxidation. *Cell.* 2008;133:462–474. doi: 10.1016/j.cell.2008.02.048

32. Mattiazzi A, Mundiña-Weilenmann C, Guoxiang C, Vittone L, Kranias E. Role of phospholamban phosphorylation on Thr17 in cardiac physiological and pathological conditions. *Cardiovasc Res.* 2005;68:366–375. doi: 10.1016/j.cardiores.2005.08.010

33. Ishida A, Kameshita I, Okuno S, Kitani T, Fujisawa H. A novel highly specific and potent inhibitor of calmodulin-dependent protein kinase II. *Biochem Biophys Res Commun.* 1995;212:806–812. doi: 10.1006/bbrc.1995.2040

34. Braun JL, Hamstra SI, Messner HN, Fajardo VA. SERCA2a tyrosine nitration coincides with impairments in maximal SERCA activity in left ventricles from tafazzin-deficient mice. *Physiol Rep.* 2019;7:e14215. doi: 10.14814/phy2.14215

35. Respress JL, van Oort RJ, Li N, Rolim N, Dixit SS, deAlmeida A, Voigt N, Lawrence WS, Skapura DG, Skårdal K, et al. Role of RyR2 phosphorylation at S2814 during heart failure progression. *Circ Res.* 2012;110:1474–1483. doi: 10.1161/CIRCRESAHA.112.268094

36. van Oort RJ, McCauley MD, Dixit SS, Pereira L, Yang Y, Respress JL, Wang Q, De Almeida AC, Skapura DG, Anderson ME, et al. Ryanodine receptor phosphorylation by calcium/calmodulin-dependent protein kinase II promotes life-threatening ventricular arrhythmias in mice with heart failure. *Circulation.* 2010;122:2669–2679. doi: 10.1161/CIRCULATIONAHA.110.982298

37. Bashir A, Bohnert KL, Reeds DN, Peterson LR, Bittel AJ, de Las Fuentes L, Pacak CA, Byrne BJ, Cade WT. Impaired cardiac and skeletal muscle bioenergetics in children, adolescents, and young adults with Barth syndrome. *Physiol Rep.* 2017;5:e13130. doi: 10.14814/phy2.13130

38. Dudek J, Cheng IF, Balleininger M, Vaz FM, Streckfuss-Bömeke K, Hübscher D, Vukotic M, Wanders RJ, Rehling P, Guan K. Cardiolipin deficiency affects respiratory chain function and organization in an induced pluripotent stem cell model of Barth syndrome. *Stem Cell Res.* 2013;11:806–819. doi: 10.1016/j.scr.2013.05.005

39. Gonzalvez F, D'Aurelio M, Boutant M, Moustapha A, Puech JP, Landes T, Arnauné-Pelloquin L, Vial G, Taleux N, Slomianny C, et al. Barth syndrome: cellular compensation of mitochondrial dysfunction and apoptosis inhibition due to changes in cardiolipin remodeling linked to tafazzin (TAZ) gene mutation. *Biochim Biophys Acta.* 2013;1832:1194–1206. doi: 10.1016/j.bbadis.2013.03.005

40. Zhang M, Mileykovskaya E, Dowhan W. Gluing the respiratory chain together. Cardiolipin is required for supercomplex formation in the inner mitochondrial membrane. *J Biol Chem.* 2002;277:43553–43556. doi: 10.1074/jbc.C200551200

41. Pfeiffer K, Gohil V, Stuart RA, Hunte C, Brandt U, Greenberg ML, Schägger H. Cardiolipin stabilizes respiratory chain supercomplexes. *J Biol Chem.* 2003;278:52873–52880. doi: 10.1074/jbc.M308230200

42. Hsu P, Liu X, Zhang J, Wang HG, Ye JM, Shi Y. Cardiolipin remodeling by TAZ/tafazzin is selectively required for the initiation of mitophagy. *Autophagy.* 2015;11:643–652. doi: 10.1080/15548627.2015.1023984

43. Anderson ME, Brown JH, Bers DM. CaMKII in myocardial hypertrophy and heart failure. *J Mol Cell Cardiol.* 2011;51:468–473. doi: 10.1016/j.yjmcc.2011.01.012

44. Bezzerides VJ, Prondzynski M, Carrier L, Pu WT. Gene therapy for inherited arrhythmias. *Cardiovasc Res.* 2020;116:1635–1650. doi: 10.1093/cvr/cvaa107

45. Steinberg SF. Oxidative stress and sarcomeric proteins. *Circ Res.* 2013;112:393–405. doi: 10.1161/CIRCRESAHA.111.300496

46. Eisner DA, Caldwell JL, Trafford AW, Hutchings DC. The control of diastolic calcium in the heart. *Circ Res.* 2020;126:395–412.

47. Tohyama S, Hattori F, Sano M, Hishiki T, Nagahata Y, Matsuura T, Hashimoto H, Suzuki T, Yamashita H, Satoh Y, et al. Distinct metabolic flow enables large-scale purification of mouse and human pluripotent stem cell-derived cardiomyocytes. *Cell Stem Cell.* 2013;12:127–137. doi: 10.1016/j.stem.2012.09.013

48. Sharma A, Toepfer CN, Schmid M, Garfinkel AC, Seidman CE. Differentiation and contractile analysis of GFP-sarcomere reporter hiPSC-cardiomyocytes. *Curr Protoc Hum Genet.* 2018;96:21.12.1–21.12.12. doi: 10.1002/cphg.53

49. Sun G, Yang K, Zhao Z, Guan S, Han X, Gross RW. Matrix-assisted laser desorption/ionization time-of-flight mass spectrometric analysis of cellular glycerophospholipids enabled by multiplexed solvent dependent analyte-matrix interactions. *Anal Chem.* 2008;80:7576–7585. doi: 10.1021/ac801200w

50. Xu Y, Phoon CK, Berno B, D'Souza K, Hoedt E, Zhang G, Neubert TA, Epand RM, Ren M, Schlame M. Loss of protein association causes cardiolipin degradation in Barth syndrome. *Nat Chem Biol.* 2016;12:641–647. doi: 10.1038/nchembio.2113

51. Oda T, Yang Y, Uchinoumi H, Thomas DD, Chen-Izu Y, Kato T, Yamamoto T, Yano M, Cornea RL, Bers DM. Oxidation of ryanodine receptor (RyR) and calmodulin enhance Ca release and pathologically alter, RyR structure and calmodulin affinity. *J Mol Cell Cardiol.* 2015;85:240–248. doi: 10.1016/j.yjmcc.2015.06.009

52. Yang J, Zhang R, Jiang X, Lv J, Li Y, Ye H, Liu W, Wang G, Zhang C, Zheng N, et al. Toll-like receptor 4-induced ryanodine receptor 2 oxidation and sarcoplasmic reticulum Ca2+ leakage promote cardiac contractile dysfunction in sepsis. *J Biol Chem.* 2018;293:794–807. doi: 10.1074/jbc.M117.812289

53. Terentyev D, Györke I, Belevych AE, Terentyeva R, Sridhar A, Nishijima Y, de Blanco EC, Khanna S, Sen CK, Cardounel AJ, et al. Redox modification of ryanodine receptors contributes to sarcoplasmic reticulum Ca2+ leak in chronic heart failure. *Circ Res.* 2008;103:1466–1472. doi: 10.1161/CIRCRESAHA.108.184457

54. Guo A, Song LS. AutoTT: automated detection and analysis of T-tubule architecture in cardiomyocytes. *Biophys J.* 2014;106:2729–2736. doi: 10.1016/j.bpj.2014.05.013

55. von Gise A, Lin Z, Schlegelmilch K, Honor LB, Pan GM, Buck JN, Ma Q, Ishiwata T, Zhou B, Camargo FD, et al. YAP1, the nuclear target of Hippo signaling, stimulates heart growth through cardiomyocyte proliferation but not hypertrophy. *Proc Natl Acad Sci U S A.* 2012;109:2394–2399. doi: 10.1073/pnas.1116136109

56. Agah R, Frenkel PA, French BA, Michael LH, Overbeek PA, Schneider MD. Gene recombination in postmitotic cells: targeted expression of Cre recombinase provokes cardiac-restricted, site-specific rearrangement in adult ventricular muscle in vivo. *J Clin Invest.* 1997;100:169–179. doi: 10.1172/JCI119509